DOI: 10.1002/((please add manuscript number))

Article type: Communication

Micron-Scale Patterning of High Quantum Yield QD-LEDs

Giovanni Azzellino, Francesca S. Freyria, M. Nasilowski, Moungi G. Bawendi and Vladimir Bulović**

Dr. G. Azzellino, Prof. V. Bulović

Research Laboratory of Electronics, Massachusetts Institute of Technology, 77 Massachusetts Avenue, Cambridge MA 02139

Prof. V. Bulović

Department of Electrical Engineering and Computer Science, Massachusetts Institute of Technology, 77 Massachusetts Avenue, Cambridge MA 02139

E-mail: mozart87@mit.edu, bulovic@mit.edu

Dr. F. S. Freyria, Dr. M. Nasilowski, Prof. M. G. Bawendi

Department of Chemistry, Massachusetts Institute of Technology, 77 Massachusetts Avenue, Cambridge MA 02139

Keywords: inkjet printing, quantum dots, LEDs, nanopatterning, electroluminescence

Abstract

Micron-scale resolution patterning of colloidal quantum dots (QDs) is demonstrated by adopting inkjet printing as a technique that is solvent and room temperature compatible, maintains optical and electronic properties of printed QD films, and results in minimal materials waste during the deposition process. With a combination of solvent engineering and substrate patterning single prints of PbS-CdS core-shell QDs (with peak photoluminescence emission at λ = 1270 nm wavelength) are deployed to form QD films of nanoscale-thickness, with regular micron-scale patterns. Inkjet printing of infrared QD films is chosen as a case study for manufacture of QD-LEDs, and demonstrate devices with a record peak external quantum efficiency in excess of 2% that is finally comparable with state-of-the-art spin-coated prototypes.

Main text

Colloidal quantum dots (QDs) are solution-processable semiconductor nanocrystals with tunable emission and absorption spectrum both in the visible[1] and in the infrared[2]. Films of QD have been suggested for use as active layers in a variety of optoelectronics devices, including LEDs[3–11], solar cells[12,13], FETs[14,15], and photodetectors[16,17]. In particular, the need in information display technologies for spectrally-narrow light sources with saturated light emission has motivated the research efforts in QD electroluminescence[1,18] over the last two decades[19–21],[22]. The need for pixelated display structures also led to research efforts in patterning of QD thin films[23–26], yet the realization of efficient, patterned QD-LEDs remains challenging[24,27], given the difficulty of dispersing QDs into regular patterns without hampering their optical and electronic properties when deployed in a thin film[26]. In the present work, we show that QDs can be deployed into thin film patterns with micron-scale resolution, and nano-scale film thickness control, forming the emissive layer of infrared QD-LEDs with 2% external quantum efficiency (EQE). Such devices, manufactured by inkjet printing, exhibit EQE similar to that reported in literature[8] for un-patterned QD-LEDs, manufactured by spin-coating, and adopting same type of emissive core-shell QDs with photoluminescence peak emission at 1250 nm wavelength. The same print-fabrication approach could be generally extended to the manufacture of QD-LEDs of any color, enabling fabrication of side-by-side multicolor devices, as needed for the high-definition full-color information displays.

Colloidal QDs can be dispersed in many organic solvents, which facilitates the ease of their manufacturing into thin film structures, while also introducing a compatibility challenge when QD films are intended to form a heterojunction with films of different chemistry, as needed in QD-LEDs[1]. As a result, patterning of QD films through the established solvent-based lithography processes, has not been utilized. Therefore, to form QD-film patterns, other alternatives have to be considered, in particular additive and maskless printing approaches that bring two benefits: first, the direct deployment of patterned QD solutions onto a substrate[24], second, the drastic reduction of material load and waste during deposition[28] that is needed in large scale flat-panel display production and which cannot be achieved by spin-coating.

Printing techniques[29–31] have been extensively explored in organic electronics[32] to pattern soft semiconductors and build active devices on flexible substrates, by adopting a variety of materials: polymers[33,34], molecules[35], carbon nanotubes[36], and quantum dots[23,24,37]. Printed QD-LEDs have been recently investigated[24,38], but to date there is a gap between the electrical performances of spin-coated QD-LED prototypes and the printed ones[27,39]. This difference can be ascribed to the sensitive surface chemistry of the constituent QDs, and to the intrinsic nature of inkjet printing that makes the formation of smooth and continuous films challenging at the nanoscale[30,32]. Good morphology has been obtained for polymers or dyes dispersed in polymer matrices when printing micron-thick films[40], however, when films of nanoscale thickness are needed, occurrence of pinholes and film discontinuities is often observed [41]. The defects in such films can lead to electrical shorts across the LEDs, leading to unacceptably low fabrication yields[42].

Depending on the structure and the chemical modifications made to the emissive QDs, QD-LEDs with high quantum yield contain either one or few monolayers of QDs, with each monolayer a few nanometers in thickness[6,8,43], or a thick QD film[44,45]. In particular, a very recent work[45] reports infrared QD-LEDs with record EQE of 8% in the infrared by adopting a composite blend of QDs and

ZnO[45]. However, given the high complexity of this latter device structure, one possible challenge associated with the scaled-up production of it could be the sequential solvent-based processing of deposited layers, where the solvent used in the deposition of the over-layers could affect the layers underneath[41]. In view of patterning the printed QD-LEDs a simpler device architecture[1], with limited number of solution-processed steps, is preferable, given the challenge of stacking multiple solution-processed layers by inkjet printing [34,41], and the delicate chemistry of QDs[1]. The so-called type-IV structure[19] is also advantageous in terms of QD material load: monolayer-based QD-LEDs with high EQE, both in the visible[43] and in the infrared[8], reduce the overall material use of QDs[44,45]. However, high precision in the fabrication of the QD layer thickness and morphology is required to ensure consistent and controlled exciton formation and avoidance of deleterious charge buildup at defect sites[19].

QD-LEDs reported in this study adopt core-shell PbS-CdS QDs, with photoluminescence (PL) peak emission at λ = 1270 nm, corresponding to a QD energy gap of E_g = 0.97 eV and a QD diameter of 7 nm (see TEM images in Figure S1). These QDs are chosen due to their high PL quantum yield (of 50%). The shell growth is accomplished by cation exchange[46] according to the procedure detailed in the Experimental Section and reported elsewhere[8]. Devices studied here are based on the 'type-IV' hybrid inverted structure[1,19]. This QD-LEDs are bottom-emitting through the transparent cathode, with the QD film sandwiched between an inorganic electron transport layer (ETL) and an organic hole transport layer (HTL), as shown in Figure 2b. The details about the sample manufacturing are provided in the Experimental Section.

For printing of QD layers, we use a piezoelectric nozzle ink-jet printer, Fujifilm Dimatix 2800, equipped with a custom-made reservoir designed to minimize the material load (Figure S4), as compared to the commercial cartridges (see Supporting Information). Different geometries of printed films can be realized by merging the ink-jet-printed droplets in different patterns in order to form

continuous lines, pads or a spotted film. The spacing between adjacent printed droplets, lines, or the number of overlaid printing steps can be tuned to control the thickness of the patterned film without significant change in the lateral dimensions[24]. We first demonstrate the patterning capability by printing a pattern of luminescent QDs on a 10 cm by 10 cm glass substrate, forming an image that glows when illuminated with UV light, as shown in **Figure 1**. This pattern is realized with commercial core-shell CdSe-CdS QDs (from QDVision Inc.), dispersed in a toluene solution.

High quantum yield QD-LEDs (both in the visible and in the infrared) based on monolayer-thick QD film[8,43] represent a suitable device template to address the QD-LED patternability, given their ease of fabrication[1] and the reduced material load associated with their manufacturing[8,43]. However the formation of a QD monolayer is challenging to consistently control in a printing process[47]. In the fabrication of QD-LEDs it is also crucial to maintain the energy band alignment between the neighboring layers, which are set both by the surface chemistry of constituent materials and by the dipoles at interfaces, both of which can be affected by the fabrication process[1,43]. Either a spotted QD film[27,39] or voids in the QD film can lead to reduced EQE as the electric current is more likely to flow from the ETL to the HTL through the voids, given the smaller resistance exhibited by this path as compared to the one comprising the QD film in between. In light of these fabrication challenges, even though bright QD-LEDs [6–8,44,45,48] have been recently reported through spin casting, the EQE reported for patterned devices is usually not reaching the current state-of-the-art of spin-coated prototypes[24,27,39,49]. We surmise that the causes are the difficulty in controlling the thickness of the printed QD layer[27], the roughness of printed films reported so far[24,38], and the lack of electrical insulation between the active pixelated devices and the rest of the substrate[24,39].

In our demonstration, we define the area of individual active QD-LED regions by introducing a periodic insulating photoresist pattern with 100 μm pitch, limiting the opportunity to generate

inadvertent shorts through the large-area film. The size of the photoresist openings (50 μm) matches the dimensions of the printed droplet, obviating the possibility to re-dissolve the once-printed film by the subsequent deposition and minimizing the coffee-ring effect[41]. Indeed, the coffee-ring effect is the dominant cause of discontinuity, roughness, and non-uniformity in ink-jet printed films[30,41] and could be expected to have a deleterious impact on the morphology of QD films whose thickness is on the scale of few nanometers.

Also of note is the high surface energy of the ZnO layer, serving as ETL and sitting underneath the QD film, that forms a contact angle of 6° with our printed QD solutions, as measured by telescope-goniometer, and drives the uncontrolled spreading of the QD solution that can lead to pinholes in the final QD film. Surface energy reduction, either by a mild fluorinated plasma[50] or silanization[51], has been previously used to confine the footprint of the printed film and curtail the coffee-ring effect[40]. Unfortunately, we observed that the necessary prolonged exposure of ZnO films to ambient air for such functionalization of the samples results in undesired pinholes in the ZnO films, (Figure S7). These findings further led to our choice of introducing the periodic insulating photoresist pattern on top of the cathode, generating wells that controllably limit the QD solution spreading.

The array pattern of photoresist wells on the ITO cathode was fabricated with a positive tone resist, diluted in order to get the final thickness of the resist of 100 nm (see Figure S3) compatible with the overall thickness of ~ 400 nm of the final devices (shown in **Figure 2**). The patterned photoresist is not lifted off from the samples. After a bake in air at 70°C, QD-LED fabrication is fully done in a controlled inert environment, with no need to expose the samples to ambient conditions (see details in the Experimetal Section).

The QD solution is deployed by ink-jet printing in the shaped wells after spinning a ZnO NPs solution over the entire sample. The size of the wells is big enough (50 μm) to not affect the average thickness

of the ZnO in the well. As measured by AFM, the ZnO film taken across different wells is 45 nm ± 5 nm thick, same as for the spin-coated prototypes.

Although the wells provide good confinement and prevent the uncontrolled spreading of the QD solution, the QD film morphology still exhibits non-uniformities, thus requiring additional optimization. Upon considerantions on the buildup of a surface tension gradient[30,39–41] and the solubiliy of QDs in organic solvents[27] we engineered a QD-based ink (more details are available in the Supporting Information) to consistently pattern continuous films of QDs over the array of 50μm photoresist wells covering large area (few mm^2) and down to few nanometers in thickness, an example of which is shown in Figures 1b-c. The thickness of the QD layer has been probed with AFM for all of the printed samples. In case of the monolayer film, we measure 8 nm ±1 nm thickness, as shown in Figure 1c. These data have been confirmed by optical interferometry.

Figure 2 reports the J-V (e), EQE (f) and radiance (g) of three sets of QD-LEDs, based on inkjet-printed QDs with different thicknesses, accounting for the three different concentrations adopted for their manufacturing (4, 8, and 12 mg/mL). The electroluminescence (EL) spectrum collected from devices biased at 4V is reported in Figure 2d. EQE and radiance are calculated according to Supran, *et al.*[8] The current density is collected from an array of 121 devices patterned over 1.21 mm^2. Dependence of the current density on QD thickness is shown in the J-V plot (Figure 2e) where the leakage current is larger for devices with thinner QD films. We also observe dependence of EQE on the QD film thickness, as expected from this kind of devices.[6,8] Indeed, thickness optimization is required in order to find the best trade-off in terms of exciton formation and charge injection, and therefore the highest EQE.[19]

EQE in excess of 2% is measured under voltage bias between 3 V and 6 V in QD-LEDs with 8 nm thick QD film, inkjet-printed onto ZnO. By taking into account the diameter of PbS-CdS QDs (pictured in the TEM of Figure S1), and comparing it with the profilometry data, we can assess that

the highest EQE is achieved in devices with one monolayer-thick QD films, as expected from literature of type-IV QDLEDs[8,43]. In particular this result is noticeably in agreement with a previous work[8] on infrared spin-coated QD-LEDs, based on PbS-CdS with same shell thickness as ours (0.7nm, as determined by the PL shift between the core-only and the core-shell QDs) and emitting in the same wavelength regime. Therefore, the different manufacturing protocol (inkjet printing vs. spin coating) does not affect the device performance (measured in terms of EQE) as long as the low roughness and thickness uniformity of the QD film can be maintained.

A closer look into the morphology of the printed QD films is provided by the AFM topographies in **Figure 3** that are taken over a single print of a monolayer-thick QD film, obtained with 8 mg/mL solution, inkjet printed on the stack of ITO/ZnO. The cross-section (Figures 3a-b) measured across two wells, one empty and the other one filled out with QDs, confirms the QD layer thickness of 8 nm. The high quality of the inkjet-printed QD film is confirmed by the low roughness and the absence of pinholes assessed by the AFM topography in Figure 3d, collected from one of the filled wells. The roughness of our QD layer film is comparable with other spin-coated QD prototypes reported in literature.[6,47] AFM topographies (Figure S2) from different QD batches (4mg/mL and 12mg/mL) look very different: low-concentrated QD solution is associated with discontinuous QD films, which may account for the higher current density at low voltage bias (Figure 2e). On thicker films (15 nm thick on average), generated by QD solution with increased QD concentration to 12 mg/mL, the roughness exceeds 5 nm and the AFM topography reports thickness variations of several nanometers. Smooth and continuous QD films, with constant thickness are beneficial for high-yield manufacture of efficient QD-LEDs, and this work demonstrates that inkjet printing is capable of such thickness control over pixel areas. New inkjet printing toolsets for OLEDs, such as those recently demonstrated by Kateeva, Inc.[52] could one day enable manufacture of inkjet-printed state-of-the-art QD-LEDs on industrial scale.

In conclusion, this work addresses the challenge of QD film patterning and advances the development of inkjet-printed QD-LEDs, as needed in the fabrication of high-quality active pixels in display applications containing QD lumophores. Core-shell PbS-CdS QDs (peak emission at λ = 1270 nm) with high photoluminescence quantum yield (~50%) are adopted as case study and embedded in a 'hybrid'[1] type-IV, bottom emitting structure, to fabricate the infrared-emitting QD-LEDs. The most efficient devices, with peak EQE in excess of 2%, are based on monolayer-thick, continuous, and ultrasmooth QD films.

Experimental Section

Synthesis: ZnO NPs and PbS-CdS QDs were synthesized according to the procedure described in the Supporting Info. The size of the QDs is estimated by the position of the lowest energy absorption peak (λ = 1270 nm) and the TEM analysis. The as-synthesized QDs were precipitated twice from solution with ethanol, redispersed into hexane the first time, and then into a mixture of hexane, octane and 1,2-dichlorobenzene (3:1:1 by vol.).

Sample preparation: Unless otherwise specified all chemicals were purchased from MilliporeSigma. CdSe-CdS QDs were provided by QDVision Inc. Half-inch D263 borosilicate glass with patterned ITO film (150 nm thick) is used as a substrate. Substrates were cleaned by sequential sonication in Micro90 (1:100 by vol. in water), water (twice), acetone (twice) and boiling isopropyl alcohol (twice). An oxygen plasma ashing step followed the cleaning procedure in order to remove any organics residuals. Lithography was performed in MIT's Microsystem Technology Laboratory to pattern the ITO film and make an array with 100 μm pitch photoresist pattern. Positive tone SPR 700 photoresist was diluted in cyclohexane (1:4 by vol.) and spun on the substrates (4000 rpm) that were then annealed at 110° C in air before UV exposure for 12 sec under MA4 mask aligner and developed for 4

seconds in CD-26. Substrates were finally annealed at 70° C in air before being transferred in a N_2-filled glovebox for the subsequent fabrication steps. The photoresist was not lifted off from the samples. The ZnO nanoparticles dispersion was filtered (0.1 μm PTFE) prior to spin coating on the samples at 2000 rpm. PbS-CdS QDs were inkjet printed on the samples by adopting a Fujifilm Dimatix 2800 equipped with 10 pL cartridge, and adopting a custom-made small ink reservoir for reduced material usage (Figure. S4). After the deployment of the QD film, samples were annealed at 150° C in a N_2-filled glovebox and then transferred and kept overnight in high vacuum (10^{-6} mTorr). Devices were completed with the deposition of 65 nm thick hole transport layer by thermal sublimation of SP-2NP (purchased from LumTec and used as received), and the thermal evaporation of the top contact MoOx/Au (8nm/100nm thick). MoOx was purchased from Alpha Aesar and used as received. Samples were finally kept overnight in high vacuum before testing.

Electrical testing and material characterization: The entire LED testing protocol was conducted in a N_2-filled glovebox. A custom-designed PCB text-fixture with spring contacts was used to bias the devices singularly (10 per chip) on the sample. The output light from the LEDs was collected with a Newport 818-IR/DB Germanium detector. Current and light power data were collected by interfacing a multiplexer, a Keithley 2626A source meter and a power meter (Newport 1830c) through Labview. Samples were sealed with TorrSeal to undergo electroluminescent measurements in a lab equipped with an InGaAs detector, cooled with liquid N_2. The external quantum efficiency and the radiance were estimated according to the calculation listed in Supran, *et al*[8].

Overall, we produced 90 devices from 3 ink batches (9 sample chips with 10 independent devices each), with most devices working and 7 devices shorted (fabrication yield of 92%).

AFM topographies were taken with AFM Dimension 3100, Veeco Instruments, Inc. Four different samples per QD concentration were scanned and the film morphology was tested at 10 different spots on each sample. The thickness data has been collected prior to cutting the QD film with a razor blade, and eventually confirmed by optical interferometry with a Wyko NT9800, Veeco Instruments, Inc.

Optical testing: Absorption spectra were collected on a Cary 5000 UV-Vis-NIR IR spectrometer (Varian). The PL emission was recorded by exciting the sample with a $\lambda = 532$ nm diode laser and collecting the emission with an InGaAs linear array detector (Princeton Instruments OMA V). Quantum yield was measured with an integrating sphere (RTC-060-SF; Labsphere). A $\lambda = 785$-nm diode laser was used to illuminate the sample. The output was collected using a calibrated germanium detector (Newport: 818-IR) through a Stanford Research Systems SR830 lock-in amplifying system. A colored glass long-pass filter at $\lambda = 850$ nm was used to block the excitation beam.

Supporting Information

Supporting Information is available from the Wiley Online Library or from the author.

Acknowledgements

This work was supported as part of the Center for Excitonics, an Energy Frontier Research Center funded by the U.S. Department of Energy, Office of Science, Office of Basic Energy Sciences under Award No. DE-SC0001088 (MIT).

M.N. (nanocrystal synthesis) was supported by the United States Department of Energy, Office of Basic Energy Sciences, Division of Materials Sciences and Engineering (Award No. DE-FG02-07ER46454).

The authors declare no competing financial interest.

The authors gratefully acknowledge the technical support from the MTL staff (Kurt Broderick and Gary Riggott) and Melany Sponseller for collecting the UPS data.

The authors also acknowledge the use of the facilities at MTL (Microsystem Technology Laboratory) and the AFM in Prof. Jing Kong's lab at MIT.

F.S.F. gratefully acknowledges MITei-ENI Fellowship under the Eni- MIT Alliance Solar Frontiers Center.

Received: ((will be filled in by the editorial staff))
Revised: ((will be filled in by the editorial staff))
Published online: ((will be filled in by the editorial staff))

References

[1] Y. Shirasaki, G. J. Supran, M. G. Bawendi, V. Bulović, *Nat. Photonics* **2012**, *7*, 13.

[2] E. H. Sargent, *Adv. Mater.* **2005**, *17*, 515.

[3] V. Wood, M. Panzer, J.-M. Caruge, J. E. Halpert, M. G. Bawendi, V. Bulović, *Opt. Photonics Adv. Energy Technol.* **2009**, WC6.

[4] V. Wood, J.-M. Caruge, J. E. Halpert, M. G. Bawendi, V. Bulović, *Conf. Lasers Electro-Optics* **2007**, CMO1.

[5] J. M. Caruge, J. E. Halpert, V. Wood, V. Bulović, M. G. Bawendi, *Nat. Photonics* **2008**, *2*, 247.

[6] B. S. Mashford, M. Stevenson, Z. Popovic, C. Hamilton, Z. Zhou, C. Breen, J. Steckel, V. Bulovic, M. Bawendi, S. Coe-Sullivan, P. T. Kazlas, *Nat. Photonics* **2013**, *7*, 407.

[7] X. Dai, Z. Zhang, Y. Jin, Y. Niu, H. Cao, X. Liang, L. Chen, J. Wang, X. Peng, *Nature* **2014**, *515*, 96.

[8] G. J. Supran, K. W. Song, G. W. Hwang, R. E. Correa, J. Scherer, E. A. Dauler, Y. Shirasaki, M. G. Bawendi, V. Bulović, *Adv. Mater.* **2015**, *27*, 1437.

[9] A. Castelli, F. Meinardi, M. Pasini, F. Galeotti, V. Pinchetti, M. Lorenzon, L. Manna, I. Moreels, U. Giovanella, S. Brovelli, *Nano Lett.* **2015**, *15*, 5455.

[10] Y.-N. Zhang, Y.-S. Liu, M.-M. Yan, Y. Wei, Q.-L. Zhang, Y. Zhang, *ACS Appl. Mater. Interfaces* **2018**, acsami.7b16579.

[11] Y. Yang, Y. Zheng, W. Cao, A. Titov, J. Hyvonen, J. R. Manders, J. Xue, P. H. Holloway, L. Qian, *Nat. Photonics* **2015**, *9*, 259.

[12] N. Zhao, T. P. Osedach, L.-Y. Chang, S. M. Geyer, D. D. Wanger, M. T. Binda, A. C. Arango, M. G. Bawendi, V. Bulović, *ACS Nano* **2010**, *4*, 3743.

[13] C.-H. M. Chuang, P. R. Brown, V. Bulović, M. G. Bawendi, *Nat. Mater.* **2014**, *13*, 1.

[14] D. V Talapin, C. B. Murray, *Science (80-.).* **2005**, *310*, 86.

[15] T. P. Osedach, N. Zhao, T. L. Andrew, P. R. Brown, D. D. Wanger, D. B. Strasfeld, L.-Y. Chang, M. G. Bawendi, V. Bulović, *ACS Nano* **2012**, *6*, 3121.

[16] S. a McDonald, G. Konstantatos, S. Zhang, P. W. Cyr, E. J. D. Klem, L. Levina, E. H. Sargent, *Nat. Mater.* **2005**, *4*, 138.

[17] F. Prins, M. Buscema, J. S. Seldenthuis, S. Etaki, G. Buchs, M. Barkelid, V. Zwiller, Y. Gao, A. J. Houtepen, L. D. a Siebbeles, H. S. J. van der Zant, *Nano Lett.* **2012**, *12*, 5740.

[18] J. Y. Kim, O. Voznyy, D. Zhitomirsky, E. H. Sargent, *Adv. Mater.* **2013**, *25*, 4986.

[19] G. J. Supran, Y. Shirasaki, K. W. Song, J.-M. Caruge, P. T. Kazlas, S. A. Coe-Sullivan, T. L. Andrew, M. G. Bawendi, V. Bulović, *MRS Bull.* **2013**, *38*, 703.

[20] Q. Niu, Y. Shao, W. Xu, L. Wang, S. Han, N. Liu, J. Peng, Y. Cao, J. Wang, *Org. Electron. physics, Mater. Appl.* **2008**, *9*, 95.

[21] H. M. Haverinen, R. a. Myllylä, G. E. Jabbour, *Appl. Phys. Lett.* **2009**, *94*, 073108.

[22] S. H. Shin, B. Hwang, Z. J. Zhao, S. H. Jeon, J. Y. Jung, J. H. Lee, B. K. Ju, J. H. Jeong, *Sci. Rep.* **2018**, *8*, 1.

[23] L. Kim, P. O. Anikeeva, S. A. Coe-sullivan, J. S. Steckel, M. G. Bawendi, V. Bulovic, *Nano Lett.* **2008**, *8*, 4513.

[24] B. H. Kim, M. S. Onses, J. Bin Lim, S. Nam, N. Oh, H. Kim, K. J. Yu, J. W. Lee, J. H. Kim, S. K. Kang, C. H. Lee, J. Lee, J. H. Shin, N. H. Kim, C. Leal, M. Shim, J. A. Rogers, *Nano Lett.* **2015**, *15*, 969.

[25] F. Prins, D. K. Kim, J. Cui, E. De Leo, L. L. Spiegel, K. M. McPeak, D. J. Norris, *Nano Lett.* **2017**, *17*, 1319.

[26] M. J. Hampton, J. L. Templeton, J. M. Desimone, *Langmuir* **2010**, *26*, 3012.

[27] Y. Liu, F. Li, Z. Xu, C. Zheng, T. Guo, X. Xie, L. Qian, D. Fu, X. Yan, *ACS Appl. Mater. Interfaces* **2017**, *9*, 25506.

[28] M. Caironi, E. Gili, H. Sirringhaus, *Ink-jet Print. Downscal. Org. Electron. Devices* **2012**, *2*.

[29] N. Reis, C. Ainsley, B. Derby, *J. Appl. Phys.* **2005**, *97*, 094903.

[30] B. Derby, *Annu. Rev. Mater. Res.* **2010**, *40*, 395.

[31] B. Derby, *J. Eur. Ceram. Soc.* **2011**, *31*, 2543.

[32] H. Sirringhaus, T. Shimoda, *MRS Bull.* **2003**, 802.

[33] S. Jung, A. Sou, K. Banger, D.-H. Ko, P. C. Y. Chow, C. R. McNeill, H. Sirringhaus, *Adv. Energy Mater.* **2014**, n/a.

[34] G. Azzellino, a Grimoldi, M. Binda, M. Caironi, D. Natali, M. Sampietro, *Adv. Mater.* **2013**, *25*, 6829.

[35] L. Zhou, L. Yang, M. Yu, Y. Jiang, C. F. Liu, W. Y. Lai, W. Huang, *ACS Appl. Mater. Interfaces* **2017**, *9*, 40533.

[36] O. S. Kwon, H. Kim, H. Ko, J. Lee, B. Lee, C. H. Jung, J. H. Choi, K. Shin, *Carbon N. Y.* **2013**, *58*, 116.

[37] B. Bangalore Rajeeva, L. Lin, E. P. Perillo, X. Peng, W. W. Yu, A. K. Dunn, Y. Zheng, *ACS Appl. Mater. Interfaces* **2017**, *9*, 16725.

[38] Y. L. Kong, I. A. Tamargo, H. Kim, B. N. Johnson, M. K. Gupta, T. W. Koh, H. A. Chin, D. A. Steingart, B. P. Rand, M. C. McAlpine, *Nano Lett.* **2014**, *14*, 7017.

[39] C. Jiang, Z. Zhong, B. Liu, Z. He, J. Zou, L. Wang, J. Wang, J. Peng, Y. Cao, *ACS Appl. Mater. Interfaces* **2016**, *8*, 26162.

[40] B.-J. de Gans, U. S. Schubert, *Langmuir* **2004**, *20*, 7789.

[41] A. Heinrichsdobler, J. C. Roigk, F. Schirmeier, C. J. Brabec, T. Wehlus, *Adv. Mater. Technol.* **2017**, *2*, 1.

[42] P. Calvert, *Chem. Mater.* **2001**, *13*, 3299.

[43] Y. Dong, J.-M. Caruge, Z. Zhou, C. Hamilton, Z. Popovic, J. Ho, M. Stevenson, G. Liu, V. Bulović, M. G. Bawendi, P. T. Kazlas, J. Steckel, S. A. Coe-Sullivan, *SID Symp. Dig. Tech. Pap.* **2015**, *46*, 270.

[44] Z. Yang, O. Voznyy, G. Walters, J. Z. Fan, M. Liu, S. Kinge, S. Hoogland, E. H. Sargent, *ACS Photonics* **2017**, *4*, 830.

[45] S. Pradhan, F. Di Stasio, Y. Bi, S. Gupta, S. Christodoulou, A. Stavrinadis, G. Konstantatos, *Nat. Nanotechnol.* **2018**, *14*, DOI 10.1038/s41565-018-0312-y.

[46] J. M. Pietryga, D. J. Werder, D. J. Williams, J. L. Casson, R. D. Schaller, V. I. Klimov, J. A. Hollingsworth, *J. Am. Chem. Soc.* **2008**, *130*, 4879.

[47] S. A. Coe-Sullivan, W.-K. Woo, J. Steckel, M. G. Bawendi, V. Bulović, *Org. Electron.* **2003**, *4*, 123.

[48] L. Qian, Y. Zheng, J. Xue, P. H. Holloway, *Nat. Photonics* **2011**, *5*, 543.

[49] J. S. Park, J. Kyhm, H. H. Kim, S. Jeong, J. Kang, S. E. Lee, K. T. Lee, K. Park, N. Barange, J. Han, J. D. Song, W. K. Choi, I. K. Han, *Nano Lett.* **2016**, *16*, 6946.

[50] C. W. Sele, T. von Werne, R. H. Friend, H. Sirringhaus, *Adv. Mater.* **2005**, *17*, 997.

[51] B. Arkles, *Paint Coatings Ind.* **2006**, 114.

[52] "http://kateeva.com," **n.d.**

Figure 1. a) Photoluminescence of green-emitting core-shell QDs inkjet printed on a 10cm by 10cm glass substrate. b) Optical interferometry image of a glass substrate patterned with 50µm-wide wells on a 100µm pitch, using a 100nm thick photoresist. PbS-CdS core-shell QDs are inkjet printed in some of the wells. c) Cross section taken along 'line 1' in figure (b) showing a QD-filled well next to an empty one, with the layer in the filled well corresponding to a QD film of monolayer thickness.

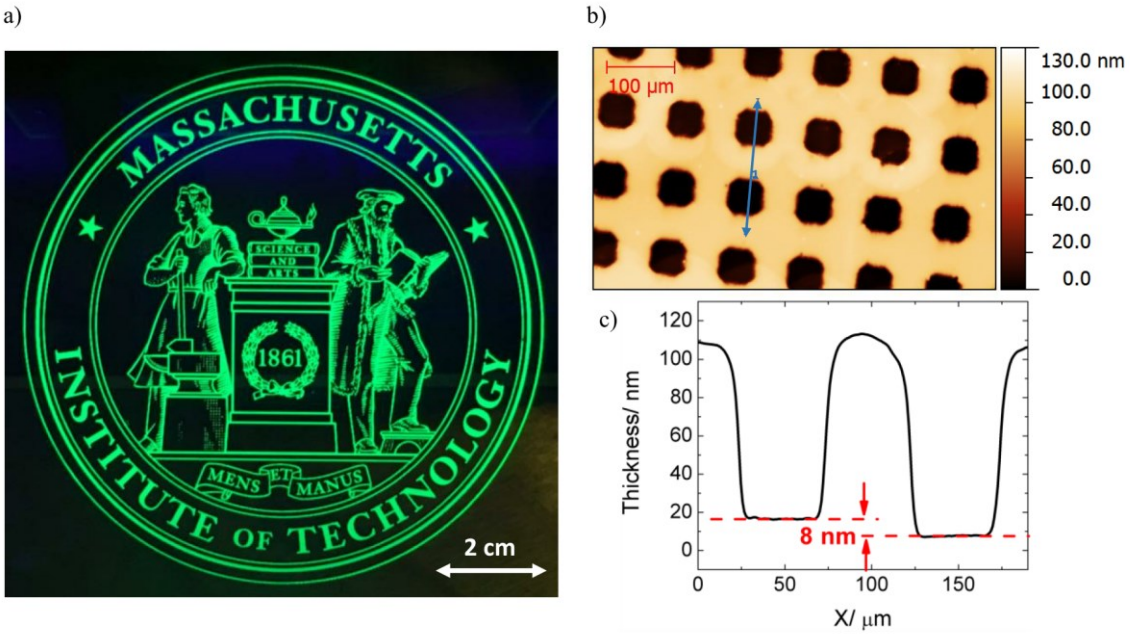

Figure 2. QD-LED manufacturing: a) Photoresist is deposited and patterned on ITO (bottom electrode) with 100 µm pitch, then ZnO NPs is spun, and finally QDs are ink-jetted in the wells defined by lithography; b) Schematic of the QD-LED structure. c) Energy level diagram of the reported QD-LEDs: HOMO and LUMO values are either taken from literature[1,8] or measured by UPS (for ZnO and SP-2NPB). **QD-LED characterization**: d) PL and EL (collected at 4V bias) of the QDs used for devices; e) J-V, f) EQE and g)

Radiance plot of QD-LEDs made out of QD solutions at different concentrations: 4mg/mL, 8 mg/mL and 12 mg/mL.

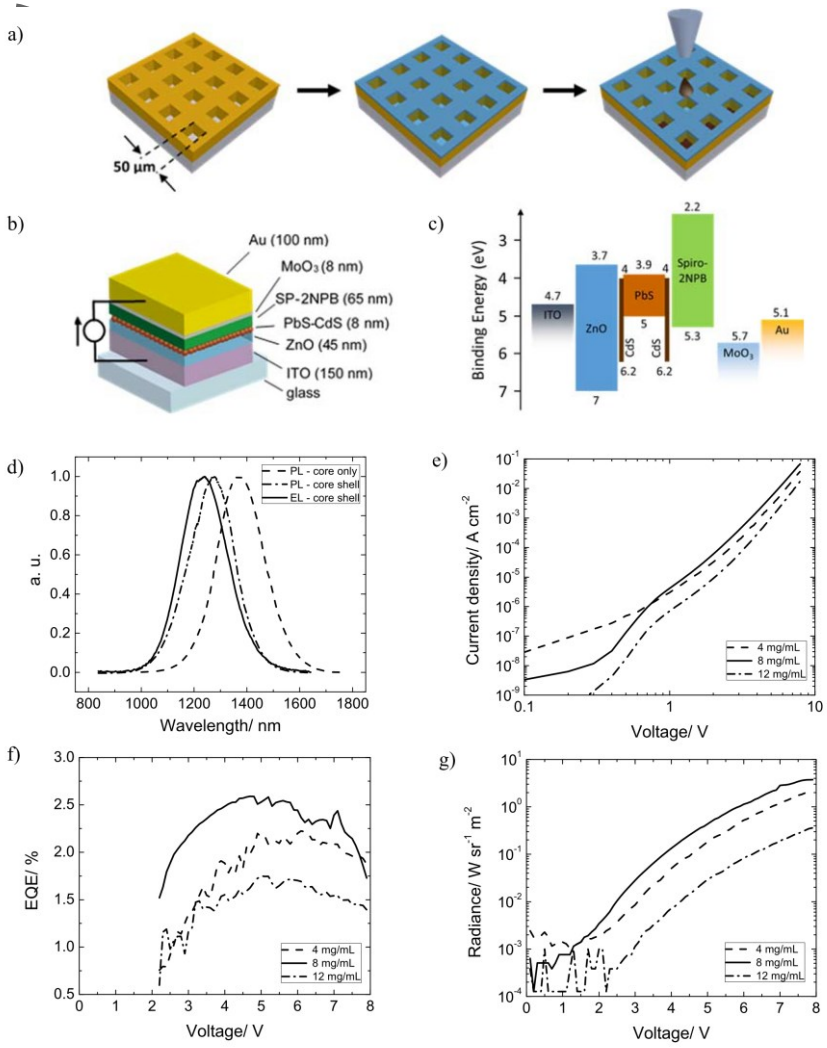

Figure 3. a) Optical interferometry micrograph of ITO covered with a patterned photoresist film. The left photoresist well along 'line 1' is filled only with ZnO, while the right well is filled with ZnO and QDs. b) Cross section height measurement of the two photoresist wells along 'line 1' show the presence of the QD layer with monolayer thickness of 8 nm. c) , d) AFM micrographs taken on ZnO and ZnO/QD films on glass/ITO substrate show film roughness of 0.6 nm and 1nm, respectively.

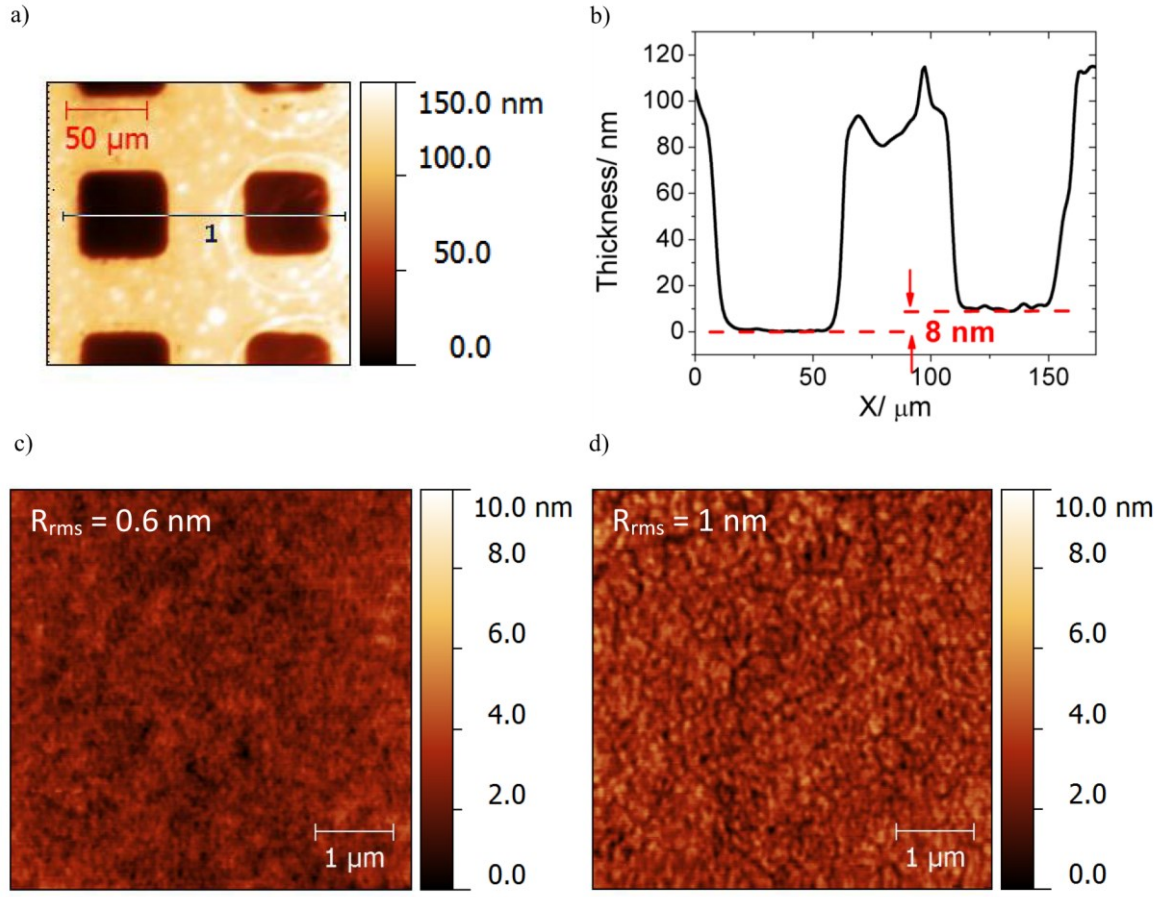

Table of Contents

Micron-scale resolution patterning of colloidal quantum dots LEDs (QD-LEDs) is reported by adopting inkjet printing, that maintains the optical and electronic properties of printed QD films, and minimizes the material waste. LEDs based on monolayer-thick layer of PbS-CdS core-shell QDs are demonstrated here, with peak photoluminescence emission at λ = 1270 nm wavelength, and high EQE in excess of 2%.

Keywords: inkjet printing, quantum dots, LEDs, nanopatterning, electroluminescence

G. Azzellino*, F. S. Freyria, M. Nasilowski, M. G. Bawendi, and V. Bulović*

Micron-Scale Patterning of High Quantum Yield QD-LEDs

ToC figure (55 mm broad × 50 mm high)